ELSEVIER

Journal of Alloys and Compounds 234 (1996) 239–243

Journal of ALLOYS AND COMPOUNDS

Magnetic incommensurability in hexagonal $HoGa_2$

D. Gignoux, D. Schmitt, F.Y. Zhang

Laboratoire de Magnétisme Louis Néel, CNRS, BP 166, 38042 Grenoble Cedex 9, France

Received 20 September 1995

Abstract

Specific heat, powder neutron diffraction experiments and magnetization measurements on a single crystal of the hexagonal $HoGa_2$ compound are presented. Below $T_N = 7.6$ K two collinear antiferromagnetic phases ($\mathbf{M} \| \mathbf{a}$ of the orthohexagonal cell) are observed: (i) a simple collinear antiferromagnetic structure with $\mathbf{Q}_1 = (0, 1, 0)$ (in the orthohexagonal cell) below $T_t = 6.5$ K; (ii) a mixing of this phase (about 36%) and of an incommensurate amplitude modulated structure (about 64%) with $\mathbf{Q}_2 = (0.123, 1, 0)$ for $T_t < T < T_N$. Below T_N smooth metamagnetic processes are observed along both directions of the easy basal plane. The second order crystal field parameter A_2^0, deduced from the shift of the reciprocal susceptibilities along and perpendicular to **c**, is significantly smaller than in the other RGa_2 compounds.

Keywords: Specific heat; Neutron diffraction; Magnetic properties; Rare earth–gallium compound

1. Introduction

$HoGa_2$ belongs to the wealthy series of RGa_2 and RAlGa hexagonal compounds (AlB_2-type structure, space group $P6/mmm$) in which the interplay between the frustration of bilinear exchange interactions and uniaxial anisotropy leads to complex field-temperature magnetic phase diagrams [1–6]. Magnetic incommensurability just below the Néel temperature often competes with commensurability which tends to be stabilized at low temperature [7], and keywords such as multistep metamagnetism, spin slip, spin flip, chaotic phase are used to characterize some features encountered in the series. Former studies on $HoGa_2$ and $DyGa_2$ indicated simple collinear antiferromagnetic structures ($\mathbf{M} \| [100]$ and $\mathbf{M} \| [010]$ respectively in the orthohexagonal notation) of propagation vector (0,1,0) below their Néel temperatures ($T_N = 8$ and 6.4 K respectively) [8,9]. Later, specific heat, resistivity and magnetization measurements on single crystal and neutron diffraction showed that in $DyGa_2$ three magnetic phases are actually stabilized below $T_N = 11.2$ K [10]. In particular, the two high temperature phases are incommensurate sine wave modulated structures, with the same propagation vector (0.134,1,0). They differ by the direction of the magnetic moments. In this paper we present specific heat measurements and neutron diffraction experiments on polycrystalline samples together with magnetization measurements on a single crystal of $HoGa_2$.

2. Specific heat measurements

The specific heat of $HoGa_2$ was measured using the a.c. calorimetry technique, at temperatures ranging from 1.7 to 40 K. This is shown in Fig. 1 together with

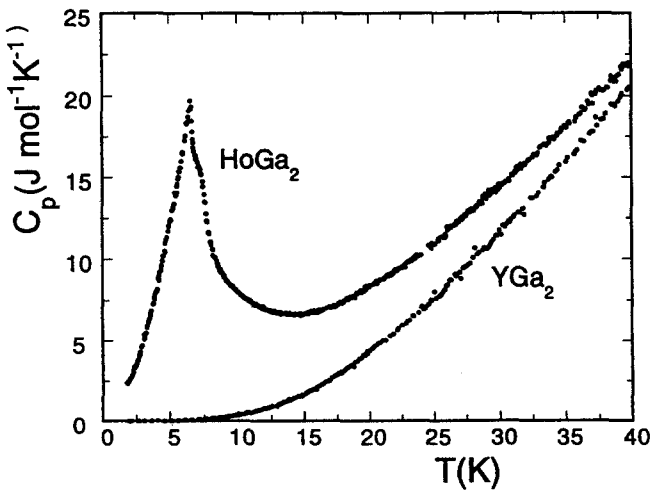

Fig. 1. Specific heat of $HoGa_2$ and YGa_2.

SSDI 0925-8388(95)02120-5

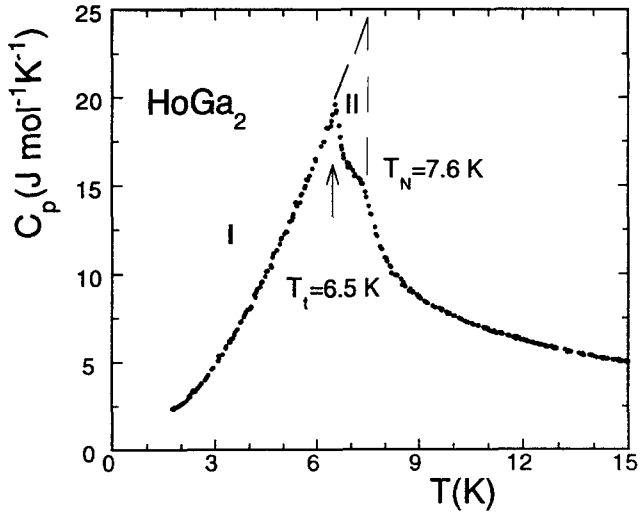

Fig. 2. Magnetic contribution to the specific heat of $HoGa_2$.

that of the non-magnetic compound YGa_2. The magnetic contribution of $HoGa_2$ is obtained by directly subtracting the specific heat of this latter compound. Indeed, the correction of Ho and Y masses by using the two Debye temperature model [11] leads to overestimation of the phonon contribution in $HoGa_2$. This magnetic contribution is shown in Fig. 2. A peak of 20 J K^{-1} mol^{-1} is observed at 6.5 K (T_t). However, a less marked anomaly is visible at a slightly higher temperature. As confirmed below, this latter anomaly is associated with the ordering temperature. From the inflexion point of this anomaly the value $T_N = 7.6$ K is obtained. No hysteresis is observed. At T_N the entropy reaches R ln (3.6). Above T_N a noticeable magnetic contribution to the specific heat remains but no clear Schottky anomaly can be detected.

3. Neutron diffraction

Neutron diffraction experiments on a powder sample were performed at the Siloé reactor, CEN Grenoble. The wavelength was 2.474 Å. Spectra were obtained at 1.8, 6.2, 6.8, 7.3, 7.5 and 15 K. Fig. 3 shows the neutron diffraction patterns obtained at 15 K, i.e. in the paramagnetic state, and the differences between those obtained at 1.8 and 7.3 K and that carried out at 15 K.

At 15 K the diagram is characteristic of the crystallographic structure. Using a Fermi length of 0.85×10^{-12} cm and 0.72×10^{-12} cm for Ho and Ga respectively, the comparison between observed and calculated intensities led to the calibrating factor and to a reliability factor $R = \Sigma\ |I_{obs} - I_{cal}| / \Sigma\ I_{obs}$ of 14%.

The 1.8–15 K difference pattern (Phase I) is indexed with the propagation vector $\mathbf{Q}_1 = (0, 1, 0)$, i.e. (0,1/2,0)

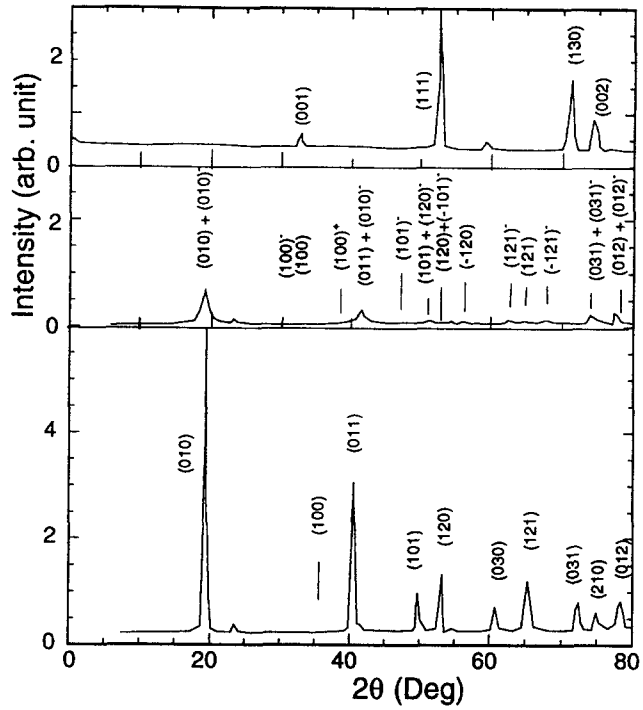

Fig. 3. Neutron diffraction patterns of $HoGa_2$: diagram at 15 K and differences between diagrams at 1.8 K and 7.3 K and the 15 K diagram. Indexation is given in the orthohexagonal system. $(hkl)^{\pm}$ reflections correspond to $(h \pm \tau,k,l)$ points of the reciprocal lattice with $\tau = 0.123$.

in hexagonal notation, in agreement with former studies [8]. This low-temperature diagram can be interpreted with the same magnetic structure as that previously determined [8]. This collinear structure is shown in Fig. 4: Ho moments are along the **a** axis of the orthohexagonal cell, i.e. perpendicular to the propagation vector, and reach 8.8 μ_B. The comparison between the calculated and observed intensities leads to a reliability factor of 8.2%.

The intensities of the 7.3–15 K difference pattern

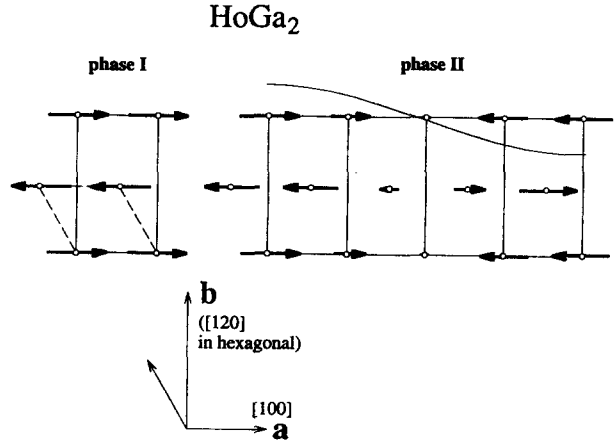

Fig. 4. Magnetic structure of $HoGa_2$ below and above T_t.

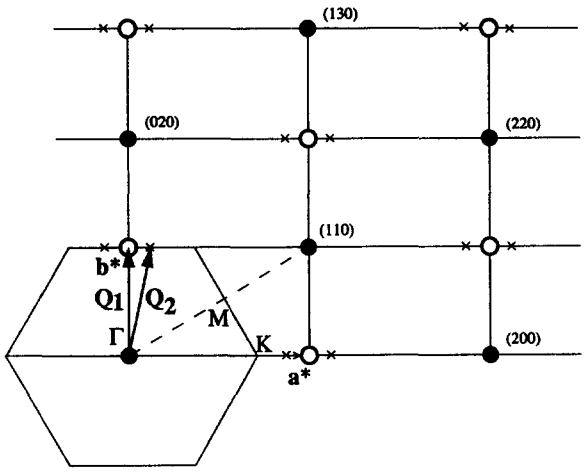

Fig. 5. Reciprocal lattice of $HoGa_2$. Full circles are the nuclear peaks. Open circles are magnetic reflections in the low temperature phase associated with the (0,1,0) propagation vector in the orthohexagonal cell. Crosses are magnetic reflections above T_t associated with the propagation vector $\mathbf{Q}=(0.123, 1, 0)$ still in the orthohexagonal cell.

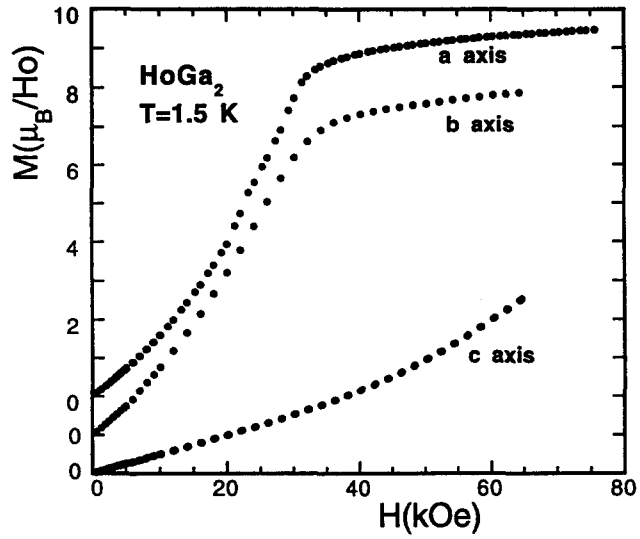

Fig. 6. Low temperature magnetization processes in $HoGa_2$ along the three main symmetry axes of the orthohexagonal cell.

(Phase II) are weak on account of the closeness of the ordering temperature. Two propagation vectors, arising from a phase mixing, are necessary to index this pattern. One part of the peaks are indexed with the low temperature propagation vector, namely $\mathbf{Q}_1=(0, 1, 0)$. The other peaks can be indexed with a slightly different incommensurate propagation vector $\mathbf{Q}_2=(\tau, 1, 0)$ in the orthorhombic cell with $\tau=0.123$ (Fig. 5). Assuming the same average magnetic moment for both phases, the refinement of the peaks associated with the incommensurate phase leads to an amplitude modulated structure with moments always along **a** and a maximum Ho moment around 3.8 μ_B and to an amount of 64% of the modulated phase. On account of the error bars of the peaks due to their weakness, the reliability factor in only 20%. In order to describe the modulated phase shown in Fig. 4, it is more simple to use the equivalent propagation vector on the line ΓK of the reciprocal space (Fig. 5), $\mathbf{Q}_2=(1-\tau, 0, 0)$ which is out of the first Brillouin zone. In that case the structure corresponds to a longitudinal modulation of the low temperature phase along the [100] direction. The pattern performed at 7.5 K, although still weaker, seems to indicate that the relative amount of both phases does not significantly changes up to T_N.

4. Magnetization measurements

4.1. Low temperature magnetization processes

Fig. 6 shows the magnetization processes of $HoGa_2$ at 1.5 K along the three main symmetry axes **a**, **b** and **c** of the orthorhombic unit cell. The **c** axis is the hard magnetization direction. However, the magnetization along this axis is not quite linear and allows prediction of a transition above 70 kOe. The magnetization in a field of 64 kOe reaches 4.5 μ_B/Ho. Along **a** and **b** the magnetization curves are very similar, and a smooth transition is observed around 30 kOe. Along **a** a weaker transition occurs around 20 kOe. In a field of 64.4 kOe, magnetization reaches 9.4 and 8.9 μ_B/Ho along **a** and **b** respectively. This shows that **a** is the easy magnetization direction, in agreement with neutron diffraction results. Magnetization curves do not significantly change up to T_N. These magnetization processes are rather different from those measured on $DyGa_2$, which has a rather similar low temperature structure [10]. Indeed, in this latter compound, numerous, rather sharp, metamagnetic transitions are observed leading to a complex field-temperature phase diagram along both symmetry directions of the basal plane. The origin of this difference is discussed below.

4.2. Paramagnetic susceptibilities

Fig. 7(a) shows the reciprocal susceptibilities of $HoGa_2$ along and perpendicular to the **c** axis. Above 100 K, a Curie–Weiss behaviour is observed, with an effective magnetic moment $\mu_{eff}=10.6$ μ_B, in agreement with the free Ho^{3+} ion value. The deduced paramagnetic Curie temperatures are $\theta_p^{\perp}=4$ K and $\theta_p^{\parallel}=-14$ K.

The low field susceptibility along **a** and at low temperature is shown in Fig. 7(b). A very broad maximum is observed around T_N, but no clear anomaly can be detected at T_t. This can arise from: (i) the persistence of the low temperature phase above T_t; (ii) the closeness of T_N.

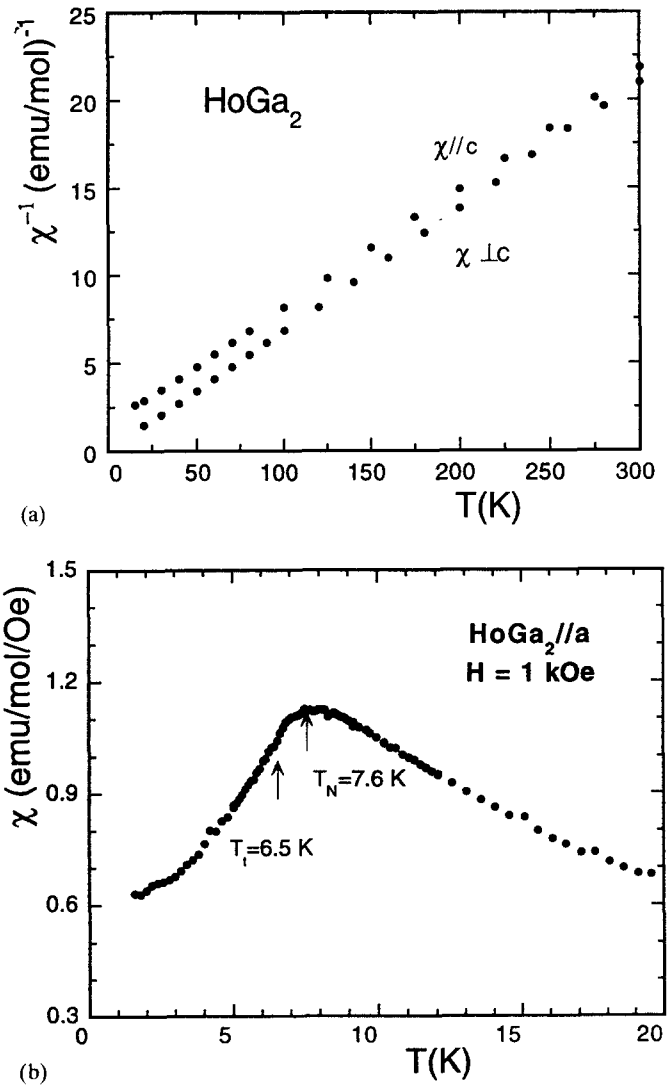

Fig. 7. (a) Reciprocal magnetic susceptibility of $HoGa_2$ along and perpendicular to the **c** axis. (b) The low temperature susceptibility of $HoGa_2$ along the **a** axis measured in a 1 kOe applied field.

5. Discussion

Thanks to specific heat and neutron diffraction, it has been possible to gain evidence of an incommensurate amplitude modulated structure in a small temperature range just below T_N. Thus $HoGa_2$ joins the (ever growing) list of compounds which are incommensurately modulated just below T_N and transform into an equal moment structure at low temperature. It is worth noting that $HoGa_2$ and $DyGa_2$ have the same low temperature commensurate propagation vector and almost the same high temperature incommensurate one. Some comments can be made about this incommensurate propagation vector: (i) it should correspond to the true maximum of the Fourier transform $J(\mathbf{q})$. It is worth noting that this maximum lies in the same region of the **q** space (KM line in Fig. 5) for the RGa_2 compounds with heavy rare earths as stressed in Ref. [12]; (ii) such a propagation vector can be stabilized only if the exchange interactions between third nearest neighbours within the basal plane are taken into account; (iii) the transition toward a simple commensurate propagation vector is a general trend which can be accounted for considering the true **q**-dependence of $J(\mathbf{q})$ in uniaxial systems [7].

The thermal variation of the specific heat below T_t is in agreement with an equal moment system, and its extension (dashed line in Fig. 2) up to T_N would lead to a discontinuity at this temperature of a good order of magnitude for this type of structure. The decrease of the specific heat between T_t and T_N, as well as the reduction of the discontinuity at T_N (actually softened by the magnetic fluctuations above T_N) are quite consistent with the existence of a high temperature modulated structure [13].

From the shift of the high temperature reciprocal susceptibilities along and perpendicular to **c** one can deduce the second order crystal field parameter $B_2^0 = \alpha_J \langle r^2 \rangle A_2^0 = 0.16K$ (α_J is the second order Stevens multiplicative factor). The value $\langle r^2 \rangle A_2^0 = -72$ K is then deduced; it is particularly small compared with that of the neighbouring RGa_2 compounds. Indeed it reaches −187 K, −145 K and −193 K for R = Tb, Dy and Er respectively [14]. This relative weakness of the second order CEF parameter probably leads to a rather small overall splitting, as would be expected knowing that the magnetic entropy at 30 K is about 21 K mol^{-1} K^{-1}, i.e. R ln(12.5), whereas R ln 17 = 23.0 K mol^{-1} K^{-1}.

As noted above, a pronounced multistep metamagnetic behaviour is observed at low temperature along **a** and **b** of $DyGa_2$ which has a magnetic structure similar to that of $HoGa_2$. Actually, this behaviour of $DyGa_2$ is observed on a crystal obtained by the Czochralski technique, whereas, in contrast, on a $DyGa_2$ crystal prepared by the Bridgman technique only a smooth metamagnetic behaviour is observed along the same axes. This is well illustrated in Fig. 8, where the low temperature magnetization curves along **b** for both crystals are compared. In fact, in our installations, crystals obtained by the Bridgman technique are grown in an alumina crucible, whereas those obtained by the Czochralski method are grown in a cold crucible. So, in the former, some contamination of the alloy by the crucible does occur and leads to some inhomogeneities and defects responsible for the smoothing out of all transitions. The magnetization curves of $HoGa_2$ obtained by the Bridgman technique are quite similar to those of $DyGa_2$ prepared with the same method. It can then be concluded that the true metamagnetic process of $HoGa_2$ is probably similar to that of $DyGa_2$, leading to complicated field-temperature phase diagrams along **a** and **b**. From our crystal it is not possible to deduce these phase diagrams along

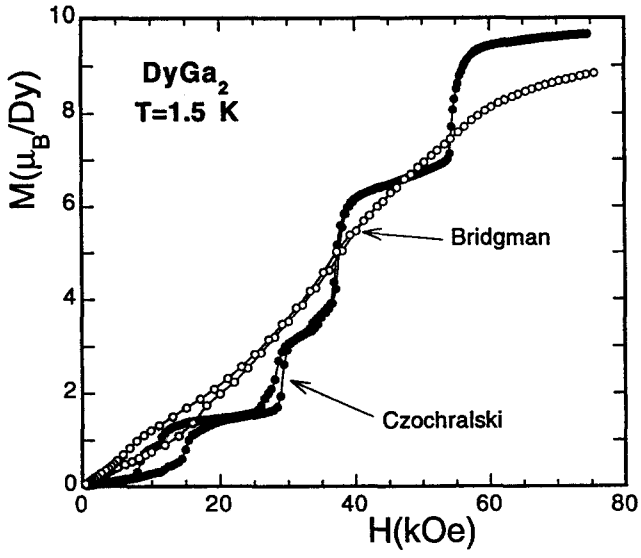

Fig. 8. $DyGa_2$: magnetization curves (in increasing and decreasing fields) measured along the **b** axis of two single crystals prepared by the Bridgman (alumina crucible) and the Czochralski (cold crucible) techniques.

each axis for $HoGa_2$. This would only be possible with a better single crystal obtained by the Czochralski technique. Unfortunately, we did not succeed in synthesizing a crystal using this method.

References

[1] D. Gignoux, D. Schmitt, A. Takeuchi, F.Y. Zhang, C. Rouchon and E. Roudaut, *J. Magn. Magn. Mater., 98* (1991) 333.
[2] A.R. Ball, D. Gignoux, D. Schmitt, F.Y. Zhang and M. Reehuis, *J. Magn. Magn. Mater., 110* (1992) 343.
[3] A.R. Ball, D. Gignoux, D. Schmitt and F.Y. Zhang, Phys. Rev. B 47 (1993) 11887.
[4] A.R. Ball, D. Gignoux, A.P. Murani and D. Schmitt, *Physica B, 190* (1993) 214.
[5] A.R. Ball, D. Gignoux, D. Schmitt, F.Y. Zhang and P. Burlet, *J. Magn. Magn. Mater., 130* (1994) 317.
[6] A.R. Ball, D. Gignoux, J. Rodriguez Fernandez and D. Schmitt, *J. Magn. Magn. Mater., 137* (1994) 281.
[7] D. Gignoux and D. Schmitt, *Phys. Rev. B, 48* (1993) 12682.
[8] B. Barbara, C. Bècle and E. Siaud, *J. Phys. (Paris) Colloq. 1, 32* (1971) 1126.
[9] T. Tsai and D. Sellmyer, *Phys. Rev. B, 20* (1979) 4577.
[10] D. Gignoux, D. Schmitt, A. Takeuchi and F.Y. Zhang, *J. Magn. Magn. Mater., 97* (1991) 15.
[11] M. Bouvier, P. Lethuillier and D. Schmitt, *Phys. Rev. B, 43* (1991) 13137.
[12] A.R. Ball, D. Gignoux, D. Schmitt and F.Y. Zhang, *J. Magn. Magn. Mater., 140–144* (1995) 1121.
[13] J.A. Blanco, D. Gignoux and D. Schmitt, *Phys. Rev. B, 43* (1991) 13145.
[14] I. Auneau, G.L.F. Fraga, D. Gignoux, D. Gignoux and F.Y. Zhang, *Physica B, 212* (1995) 351.